THE ASTROPHYSICAL JOURNAL, 353:193–199, 1990 April 10

WARM DENSE GAS IN THE REFLECTION NEBULA NGC 2023

D. T. JAFFE,[1,2] R. GENZEL,[3] A. I. HARRIS,[2,3] J. E. HOWE,[1] G. J. STACEY,[4] AND J. STUTZKI[2,3]
Received 1989 June 9; accepted 1989 September 25

ABSTRACT

We have studied the photodissociation region associated with the reflection nebula NGC 2023 by observing the $J = 2 \rightarrow 1$, $3 \rightarrow 2$, and $7 \rightarrow 6$ lines of CO, the $J = 2 \rightarrow 1$ line of $C^{18}O$ and the $^2P_{3/2} \rightarrow {}^2P_{1/2}$ transition of C^+. Southeast of the exciting star, there is a bright ridge where emission in the CO $7 \rightarrow 6$ and [C II] lines coincides with fluorescently excited H_2 emission. A dense shell of less highly excited molecular gas lies just to the southeast of the H_2 ridge. The bright, narrow CO $7 \rightarrow 6$ lines show that the warm molecular gas is hotter than the dust in NGC 2023 and make shock excitation very unlikely. Although the photodissociation region is the likely source of the CO $7 \rightarrow 6$ emission, photodissociation models can provide a satisfactory explanation for the amount of warm CO observed only if the gas densities are $\geq 10^5$ cm^{-3}. Photodissociation region models cannot explain both the CO $7 \rightarrow 6$ and the fluorescent H_2 emission if the gas is highly clumped.

Subject headings: interstellar: molecules — nebulae: individual (NGC 2023) — nebulae: reflection

I. INTRODUCTION

Photodissociation regions (PDRs) are boundary layers formed on neutral clouds wherever radiation at far-UV wavelengths (91 nm $< \lambda <$ 200 nm) impinges on their surfaces. Such layers can form at the dense interfaces between H II regions and molecular clouds, on the surfaces of reflection nebulae, in the outer portions of neutral stellar winds, and in the lower density interstellar gas. Photodissociation regions are distinguished physically by the dominant role played by far-UV radiation in determining the physical conditions, energetics, and chemistry. In our own Galaxy, the photodissociated boundaries of dense clouds near regions which have recently formed O and B stars dominate both the emission of far-IR fine structure lines from neutral or low ionization atomic species like O°, C^+, and Si^+, and emission in the submillimeter and far-IR rotational transitions of CO. In external galaxies with active ongoing star formation, it is the ensemble of these dense PDRs which produces the observed far-IR fine-structure lines (Crawford *et al.* 1985, Stacey *et al.* 1985). PDRs in these galaxies may also account for the major portion of the CO $J = 1 \rightarrow 0$ line flux (Wolfire, Hollenbach, and Tielens 1989).

Our current knowledge of PDRs comes from a series of observations over the last 10 yr of atomic fine-structure lines, CO rotational transitions, and H_2 vibrational transitions from such regions, and from detailed physical and chemical models of UV-illuminated boundaries of molecular clouds. The observations indicate that PDRs are clumpy. The length-scale for the dropoff of [C II] emission into the almost edge-on PDR in M17 SW (1–2 pc) is one to two orders of magnitude greater than would be expected from a uniform cloud (Stutzki *et al.* 1988). Howe *et al.* (1990) obtain a similar result in NGC 1977. Stutzki *et al.* (1988) show that the observed scale-length in M17 is reasonable if the C^+ lies on the outside of predominantly molecular clumps with a volume filling factor of $0.1 \rightarrow 0.3$.

Observers have also used comparisons of the 158 μm [C II] line intensity to the intensities of the 63 μm and 145 μm [O I] lines to determine the temperature and density in the PDRs. These line ratios show that the atomic gas in PDRs has temperatures between 100 and 400 K and densities of 10^4 to several 10^5 cm^{-3} (Genzel, Harris, and Stutzki 1989), although the atomic region in the reflection nebula NGC 7023 appears to have a somewhat lower density (Chokshi *et al.* 1988). There is also warm CO associated with the PDRs. The M17 SW region shows bright ($T_{MB} \simeq 85$ K), 5–7 km s^{-1} wide CO $7 \rightarrow 6$ lines over a region of ~ 1 pc extent. A multitransition CO study of M17 yields a temperature in this gas of 150–300 K and a density of 10^4–10^5 cm^{-3}, comparable to the conditions in the atomic gas (Harris *et al.* 1987*b*). Such warm, narrow line CO is present near ionized/neutral boundaries in Orion, W 51, and other sources (Schmid-Burgk *et al.* 1989; Jaffe *et al.* 1989; Stutzki *et al.* 1989), establishing a positional association of the molecular emission with PDRs but not indicating what the heating mechanism for the warm CO might be.

One-dimensional models which take into account the most important physical and chemical properties of photodissociation regions can successfully predict most of the observed line strengths (Tielens and Hollenbach 1985*a*). In these models, the dominant heat source for the gas is energetic electrons ejected from grains by the photoelectric effect and the cooling is primarily through [O I] and [C II] lines in the outer part of the PDR and by CO in the inner part. At high densities, ($n \geq 10^6$ cm^{-3}), collisional de-excitation of fluorescently excited H_2 also contributes to the heating (Tielens and Hollenbach 1985*b*; Sternberg and Dalgarno 1989). The models calculate the UV photochemistry through the region where hydrogen makes the transition from H to H_2 and carbon goes from C^+ to C° to CO and also deal with the transfer of UV radiation through the dust. While PDR models with reasonable parameters can explain the intensities of the far-IR fine-structure lines (Tielens and Hollenbach 1985*a*; van Dishoek and Black 1988; Burton, Hollenbach, and Tielens 1989), and the observed H_2 fluorescent spectrum (Black and van Dishoeck 1987; Sternberg 1988; Sternberg and Dalgarno 1989), at the densities derived from observations of PDRs in M17 and S106 (Harris *et al.* 1987*b*), they produce an order of magnitude less intensity in the submillimeter and far-IR CO lines than is observed. The problem is that the models do not predict suffi-

[1] Department of Astronomy, University of Texas at Austin.
[2] Visiting Astronomer, Infrared Telescope Facility, operated by the University of Hawaii under contract with the National Aeronautics and Space Administration.
[3] Max Planck Institute für extraterrestrische Physik.
[4] Department of Physics, University of California, Berkeley.

cient column densities of CO in the region at $A_v < 2$–4 where T_{gas} is greater than T_{dust}. Burton, Hollenbach, and Tielens (1989) have suggested, however, that the warm interface gas will produce a sufficient amount of CO cooling if the density in the PDR is very high ($n_{H_2} = 10^6$–10^7 cm^{-3}).

NGC 2023 is a well-studied reflection nebula embedded in the L1630 molecular cloud at a distance of 450–500 pc (Racine 1968; Lee 1968; de Boer 1983; we adopt $d = 475$ pc). The illuminating star, HD 37903, is type B1.5 V. The detection of emission from fluorescently excited molecular hydrogen (Gatley *et al.* 1987), of 2 μm emission from a hot ($\sim$1000 K) dust component (Sellgren, Werner, and Dinerstein 1983), and of excess flux in the *R* and *I* bands (Witt, Kraiman, and Schild 1984) toward this source show that the stellar UV interacts with the molecular cloud. From a map of the CO $J = 1 \rightarrow 0$ transition, Gatley *et al.* (1987) conclude that there is a shell of molecular material $\sim$75″ (0.17 pc) from HD 37903. At this distance, the incident far UV flux is $\sim$1000 times the interstellar radiation field value ($G_0 = 1.6 \times 10^{-3}$ ergs cm^{-2} s^{-1}, 91 nm $< \lambda <$ 300 nm; Habing 1968), or an order of magnitude below the fluxes incident on sources where we have previously observed the CO $J = 7 \rightarrow 6$ line. White *et al.* (1989) have observed the NGC 2023 region on a larger scale in the CO $J = 2 \rightarrow 1$ and $3 \rightarrow 2$ lines.

NGC 2023 is an ideal source for an examination of the heating of atomic and molecular gas in PDRs: It has a known UV source, it is known that the UV radiation is incident on the molecular cloud (from a star on the near side), the lines from molecular and neutral atomic gas are narrow ($\leq$1.5 km s^{-1}) making it easier to separate different dynamical components and to exclude the possibility of shock excitation, and a large number of observations of the nebula exist. We present here measurements of the CO $J = 2 \rightarrow 1$, $C^{18}O$ $2 \rightarrow 1$, and CO $3 \rightarrow 2$ transitions to trace the bulk of the molecular gas. We have observed the 372 μm CO $7 \rightarrow 6$ line to trace the distribution of warm molecular gas and the 158 μm C^+ $^2P_{3/2} \rightarrow {}^2P_{1/2}$ fine-structure line to trace warm neutral atomic gas in the same region. By comparing these results with existing maps of the fluorescently excited molecular hydrogen, we hope to shed light on the structure of the region, the heating of the gas and the relationship between the various carbon constituents.

II. OBSERVATIONS

We observed the 806.651 GHz CO $J = 7 \rightarrow 6$ transition with the NASA-IRTF on Mauna Kea in 1988 January using the U.C. Berkeley-MPE submillimeter heterodyne receiver (Harris *et al.* 1987*a*). The measured beam size was 34″. We measured the sky temperature at regular intervals and calculated the transmission by assuming that the physical temperature of the sky was the same as the ground temperature, and that the opacity has a linear sec (z) dependence. Our calculation allows for the difference in transmission in the signal and image sidebands and for the presence of ambient temperature blockage in the beam (Harris 1986). The zenith transmission was 27% on the night of the observations. We determined the telescope main beam efficiency (0.55) from observations of Jupiter assuming a Planck brightness temperature of 123 K, based on the observed broad-band brightness temperature (Hildebrand *et al.* 1985), corrected for PH_3 and HCN absorption in the signal and image sidebands (Lellouch, Encrenaz, and Combes 1984). We used the measured atmospheric transmission and beam efficiency to calibrate the CO $J = 7 \rightarrow 6$ lines in units of Rayleigh-Jeans main-beam brightness temperature (T_{MB}, the Rayleigh-Jeans temperature which would result from radiation from a uniform blackbody source completely filling the main beam and incident on a telescope with unity beam efficiency located outside the atmosphere). The line brightness temperature toward Orion/KL was 175 K on the resulting T_{MB} scale (Stutzki *et al.* 1989). The observations were made by chopping the secondary between the source and two positions 5′ to the east and west. The telescope pointing accuracy was better than $\pm$3″, and the boresight was known to better than $\pm$4″. The 1024 channel acousto-optical spectrometer backend had a channel spacing of 537 kHz and an effective resolution of $\sim$940 kHz (0.35 km s^{-1}). We observed at positions along a southeast to northwest scan through HD 37903 with 42″ spacings between the observed points.

We observed the 345.796 GHz CO $J = 3 \rightarrow 2$ transition in 1988 January with the University of Texas Millimeter Wave Observatory[5] 4.9 m telescope on Mount Locke. The beam size for these observations was 46″. Overall pointing uncertainties were less than $\pm$20″. We checked the sky transmission at regular intervals by making sky temperature measurements at several zenith angles. Both the $3 \rightarrow 2$ and $2 \rightarrow 1$ measurements were made in the position switching mode, alternating between observations of the source and of a reference position previously determined to be free of CO emission. In the CO $3 \rightarrow 2$ line, we covered the same southeast to northwest cross scan through HD 37903, observing at the CO $7 \rightarrow 6$ positions and at additional positions farther from the star.

We observed the 230.538 GHz $^{12}C^{16}O$ and 219.560 GHz $^{12}C^{18}O$ $J = 2 \rightarrow 1$ transitions in 1987 March with the NRAO 12 m telescope on Kitt Peak.[6] The beam size for these observations was 32″ at CO $J = 2 \rightarrow 1$ and 34″ at $C^{18}O$ $J = 2 \rightarrow 1$. Overall pointing uncertainties were less than $\pm$15″. We mapped the CO $2 \rightarrow 1$ line at 30″ intervals over a 4′ × 4′ area making repeated measurements of the central position to maintain a relative calibration within the map of better than $\pm$7%. We observed the $C^{18}O$ $2 \rightarrow 1$ line along the same southeast to northwest cut as in the CO $7 \rightarrow 6$ and $3 \rightarrow 2$ observations (at the positions of the $2 \rightarrow 1$ measurements except just southeast of the star where the observations were at half the $2 \rightarrow 1$ spacing) and at several other positions on the source.

Both the NRAO 12 m telescope at 230 GHz and the MWO 4.9 m telescope at 345 GHz have error patterns with power comparable to the power in the main beam. The 230 GHz 12 m beam has a 32″ diameter main component (forward gain 0.996) and a 510″ diameter error pattern (forward gain 0.0036; P. Jewell, personal communication). The 345 GHz MWO beam had a 46″ diameter main beam containing 60% of the power within 15′ of beam center (S. Zhou, personal communication). Corrections to the main beam temperature scale for contributions to the line power by CO emission in the error pattern are necessary with the position-switched CO $3 \rightarrow 2$ and $2 \rightarrow 1$ observations of NGC 2023 since the emission region is extended in these lines. The CO $2 \rightarrow 1$ integrated line strength distribution is $\sim$240″ east-west and very extended north-south. Maps of the $1 \rightarrow 0$ line indicate that the region extends over $\sim$15′ (Maddalena *et al.* 1985). Allowing for the presence of this extended emission in the error pattern, we multiplied the

[5] The Millimeter Wave Observatory was operated by the Electrical Engineering Research Laboratory, the University of Texas at Austin, with support from the National Science Foundation and McDonald Observatory.

[6] The National Radio Astronomy Observatory is operated by Associated Universities, Inc., under cooperative agreement AST-8814515 with the National Science Foundation.

observed CO $2 \rightarrow 1$ and $3 \rightarrow 2$ T_R^* (Kutner and Ulich 1981) values by 1.47 and 1.64, respectively, to put the lines on a Rayleigh-Jeans main beam brightness temperature scale. Using this multiplication factor, T_{MB} toward Orion/KL is 118 K in the CO $2 \rightarrow 1$ line and 125 K in the $3 \rightarrow 2$ line. If particular spectral components within the line come from a less spatially extended region than the overall line, the T_R^* values would need to be multiplied by a larger factor to scale them to T_{MB} for this component. For a 90″ source, for example, one would need to multiply the T_R^* values for the $2 \rightarrow 1$ line by 2.0 rather than 1.47.

We observed the 158 μm $^2P_{3/2} \rightarrow {}^2P_{1/2}$ fine-structure transition of C^+ along the same southeast to northwest cut in 1988 January with the U. C. Berkeley tandem Fabry-Perot spectrometer on the 0.9 m Kuiper Airborne Observatory telescope. We made the observations by fixing the scanning Fabry-Perot in 80th order at the position of the [C II] line, yielding a bandpass of 67 km s^{-1}. Integrations of 10 s were made at each on-source position with the telescope secondary switching at 30 Hz to a position 5′.7 west of the source. Since the spectral resolution was larger than the line width, the C^+ scan gives information on integrated line flux only. The full width to half-maximum of the beam was 55″ (effective beam solid angle 9×10^{-8} sr). A complete [C II] map of the NGC 2023 region will be published elsewhere (Howe *et al.* 1990).

III. RESULTS

The 372 μm CO $J = 7 \rightarrow 6$ emission from NGC 2023 is bright and comes from a gas component with a low-velocity dispersion. Figure 1 shows CO $7 \rightarrow 6$ spectra along a southeast-northwest scan through the exciting star for the reflection nebula, HD 37903. Table 1 gives the line parameters for these spectra. Figure 2*b* shows the distribution of T_{MB} (CO $7 \rightarrow 6$) along this scan and compares it to the distribution of flux in the $v = 1 \rightarrow 0$ S(1) line of H_2 measured with a 20″ beam (Gatley *et al.* 1987). A CO $7 \rightarrow 6$ point 45″ east and 45″ south of the star has been added from data taken with the UCB/MPE spectrometer on the UKIRT (beam size 25″). The CO $7 \rightarrow 6$ distribution peaks 1′ southeast of the exciting star and has a full width to half-maximum of 2′. The peak T_{MB} is 67 K. Koepf *et al.* (1982) obtain a much lower temperature for the CO $6 \rightarrow 5$ line at about the same position ($T_A^* = 20$ K). Most of the difference is a result of the spectral smoothing of ~ 3 km s^{-1} applied to the CO $6 \rightarrow 5$ profile. In addition, there may be a small amount of reference beam contamination in the CO $6 \rightarrow 5$ measurements since the reference beam was only 2′ from the source position. The CO $7 \rightarrow 6$ T_{MB} of 67 K corresponds to a Planck brightness temperature (the temperature of a blackbody with equivalent brightness, given by eq. [1]), of 85 K:

$$T_{PL} = \frac{h\nu}{k} \left\{ \ln \left[1 + \frac{h\nu}{kT_{MB}} \right] \right\}^{-1} ; \quad (1)$$

T_{PL} is then a lower limit to the excitation temperature and therefore the kinetic temperature in the line-forming region. If the CO $J = 7$ state is not thermalized or the source does not fill the beam (i.e., if it is clumpy), the kinetic temperature in the gas could be considerably higher. Figure 1 shows that the CO $7 \rightarrow 6$ lines get narrower moving southeast from HD 37903. Toward the star, $\Delta V(7 \rightarrow 6)$ is 1.8 km s^{-1} (Table 1). At 2′.1 southeast, the line is only 0.8 km s^{-1} wide (correcting the observed profile for instrumental broadening). By comparison, the thermal line width would be 0.4 km s^{-1} for $T_{gas} = 100$ K.

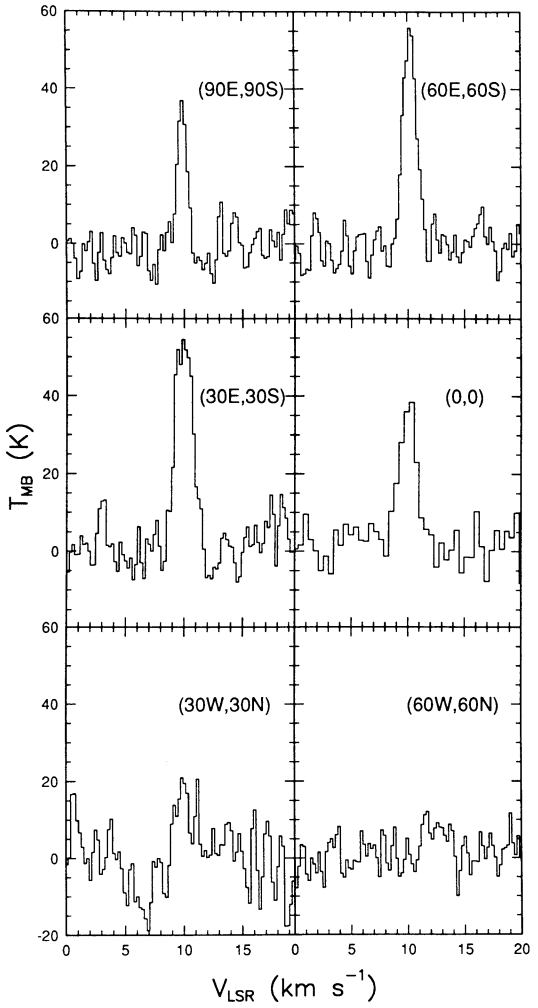

FIG. 1.—Spectra of CO $J = 7 \rightarrow 6$ in NGC 2023. The positions labeled in each spectrum are in arcseconds relative to HD 37903 (R.A. = 05^{h}39^{m}07^s.3, decl. = −02°16′58″). The vertical axis units are the Rayleigh-Jeans main beam brightness temperature of the line.

The 158 μm $^2P_{3/2} \rightarrow {}^2P_{1/2}$ line emission from C^+ is also bright and extended, and peaks southeast of HD 37903. The peak surface brightness of the [C II] line is 1.1×10^{-3} ergs cm^{-2} s^{-1} sr^{-1}. This peak surface brightness corresponds to a C^+ column density of 8×10^{17} cm^{-2} (for $T = 200$ K, $n = 3 \times 10^4$ cm^{-3}). The [C II] line flux distribution (Fig. 2*a*) peaks 0′.7 southeast of the exciting star (close to the peak of the H_2 emission) and has a full width of half-maximum of

TABLE 1

CO $J = 7 \rightarrow 6$ LINE PARAMETERS

Position[a]	T_{MB} (K)	V_{LSR} (km s^{-1})	ΔV (km s^{-1})	$\int T_{MB} dV$ (K km s^{-1})
60W, 60N	<10	...	...	<15
30W, 30N	19	10	~1.3	~25
0, 0	37	10.0	1.8	74
30E, 30S	58	10.0	1.7	96
60E, 60S	56	10.2	1.4	79
90E, 90S	38	9.9	0.9	22

[a] Offset in arcseconds relative to HD 37903 [$\alpha = 05^h39^m07^s.3$, $\delta = -02°16'58''$ (1950)].

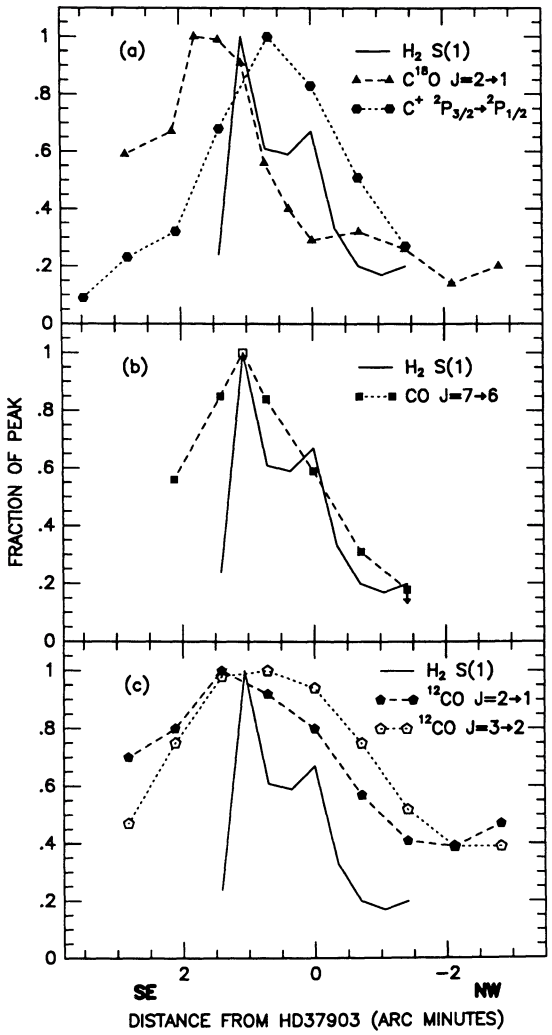

FIG. 2.—A plot of the variation of the emission from various species along a SE to NW cut passing through HD 37903, relative to the peak of the emission of each species along the cut. (*a*) The solid line plots the integrated line flux from the $v = 1 \rightarrow 0$ S(1) line of H_2 (peak flux 5.0×10^{-20} W cm^{-2} in a 19″.6 beam) from Gatley *et al.* (1987). The dashed line is the $C^{18}O$ $J = 2 \rightarrow 1$ Rayleigh-Jeans main beam brightness temperature (peak $T_{MB} = 11.0$ K) and the dotted line shows the C^+ $^2P_{3/2} \rightarrow {}^2P_{1/2}$ integrated line flux (peak flux 1.0×10^{-17} W cm^{-2} in a 55″ beam). (*b*) The dashed line gives the CO $J = 7 \rightarrow 6$ main beam brightness temperature (peak $T_{MB} = 67$ K). (*c*) The CO $J = 2 \rightarrow 1$ (peak $T_{MB} = 75$ K) and CO $J = 3 \rightarrow 2$ (peak $T_{MB} = 63$ K) main beam brightness temperature variation is shown. The beam size (FWHM) is 32″ for the CO $J = 2 \rightarrow 1$ and $C^{18}O$ $J = 2 \rightarrow 1$ observations, and 46″ for the CO $J = 3 \rightarrow 2$ observations.

2′.5. Two-dimensional mapping shows that the peak of the [C II] distribution lies along the scan shown in Figure 2 (Howe *et al.* 1989). The source is roughly circular at the 50% contour but extends north-south by more than ±3′ at the 20% level. The [C II] line is spectrally unresolved. Observations of carbon radio recombination lines from the same region (with 3′–10′ beams) indicate a line width of 1.5–2 km s^{-1} for the carbon region (Pankonin and Walmsley 1976; Knapp, Brown, and Kuiper 1977). Given this width, the peak surface brightness of the [C II] line implies a Rayleigh-Jeans brightness temperature of 70–90 K ($T_{PL} = 109$–130 K).

The largest column densities of molecular gas concentrate in a ridge just to the southeast of the H_2/CO $7 \rightarrow 6$/[C II] peak. The scan of $C^{18}O$ $J = 2 \rightarrow 1$ line temperature (Fig. 2*a*) shows that the peak of this molecular ridge is 1′.5 southeast of HD 37903. The $C^{18}O$ $2 \rightarrow 1$ emission drops to half power ~0′.5 southeast of HD 37903 but is still at a level of ~0.6 of the peak temperature ($T_{MB} = 7.5$ K) at the position 2′.8 southeast of the star. The main feature in the $C^{18}O$ $J = 2 \rightarrow 1$ line is a ~1 km s^{-1} wide spike centered at 10.2 km s^{-1} (Fig. 3). The center velocity of the $C^{18}O$ line is systematically 0.2 km s^{-1} to the red of the CO $7 \rightarrow 6$ velocity. This difference is within the uncertainties in the frequency of the $^{15}NH_3$ laser local oscillator used for the CO $7 \rightarrow 6$ measurements. At the 1 K level, there is a small pedestal of $C^{18}O$ $2 \rightarrow 1$ emission over ~3 km s^{-1}. The optically thick, low-excitation lines of CO ($J = 3 \rightarrow 2$, $2 \rightarrow 1$) peak in the same region as the $C^{18}O$ $J = 2 \rightarrow 1$ but have a broader spatial extent (Fig. 2*c*). Two-dimensional maps of the CO $J = 2 \rightarrow 1$ T_{MB} and integrated line strength show that the broad peak in the scan is part of a rim of emission east and south of HD 37903. This rim lies just to the outside of the H_2 $v = 1 \rightarrow 0$ S(1) shell source (Gatley *et al.* 1987). Figure 4 compares the two CO $2 \rightarrow 1$ maps and the H_2 map. The CO rim in Figure 4 sits upon a spatially extended emission plateau. The CO $2 \rightarrow 1$ integrated line strength is 50% or more of the peak value throughout the 4′ × 4′ area mapped. This spatially extended emission is part of a molecular cloud which runs north to the NGC 2024 cloud (Maddalena *et al.* 1986).

The CO $2 \rightarrow 1$ profiles also indicate a spectroscopic difference between the spatially extended material and the material in the southeast ridge. Figure 5*a* shows a comparison between the CO $2 \rightarrow 1$ line at a position in the ridge (90″ east and 90″ south of HD 37903) and a position at the southwest corner of the map. The profile toward the ridge is the sum of a component like the ~4 km s^{-1} wide component seen in the southwest and a ~1.2 km s^{-1} wide line. Figure 5*b* compares the profile in the southwest with a position in the northwest corner of the map. Except for a velocity shift of ~0.3 km s^{-1}, the profiles are essentially identical. The CO $2 \rightarrow 1$ profiles are similar to those in Figure 5*b* everywhere in the region away from the ridge. Figure 3 compares the CO $7 \rightarrow 6$ profile 1′.5 southeast of the star to the CO $2 \rightarrow 1$, $3 \rightarrow 2$, and $C^{18}O$ $2 \rightarrow 1$ profiles. The $7 \rightarrow 6$ line shape is very similar to the $C^{18}O$ profile but is distinctly narrower than the CO $2 \rightarrow 1$ and $3 \rightarrow 2$ lines. The difference may disappear if allowance is made for the broad-line component present in the low $-J$ lines but not apparent in the $7 \rightarrow 6$ line. An examination of the $C^{18}O$ profiles in the light of the presence of two dynamically distinct components implies that toward the peak of the ridge, ~60% of the line strength is due to the narrow component.

The spatial narrowness of the southwestern ridge seen in both the $C^{18}O$ $J = 2 \rightarrow 1$ line and in the H_2 $v = 1 \rightarrow 0$ S(1) line implies a shell or "bowl" geometry (The complete H_2 map of Gatley *et al.* [1987], which shows a shell around the exciting star, and the $R-V$ image of Witt and Schild [1988] which shows filamentary excess red emission from the ridge southeast of HD 37903 support this picture; see also Harvey, Thronson, and Gatley [1980]). Both a uniform sphere centered on HD 37903 and a uniform slab behind the star would have an emission peak at the stellar position due to increased heating. A tilted slab which is closer to HD 37903 in the southwest would have a broader emission ridge than what we observe in H_2, and no significant $C^{18}O$ enhancement. Only a local enhancement of column density, due to an edge-on shell or to a number density enhancement, can explain both the $C^{18}O$ and H_2 results.

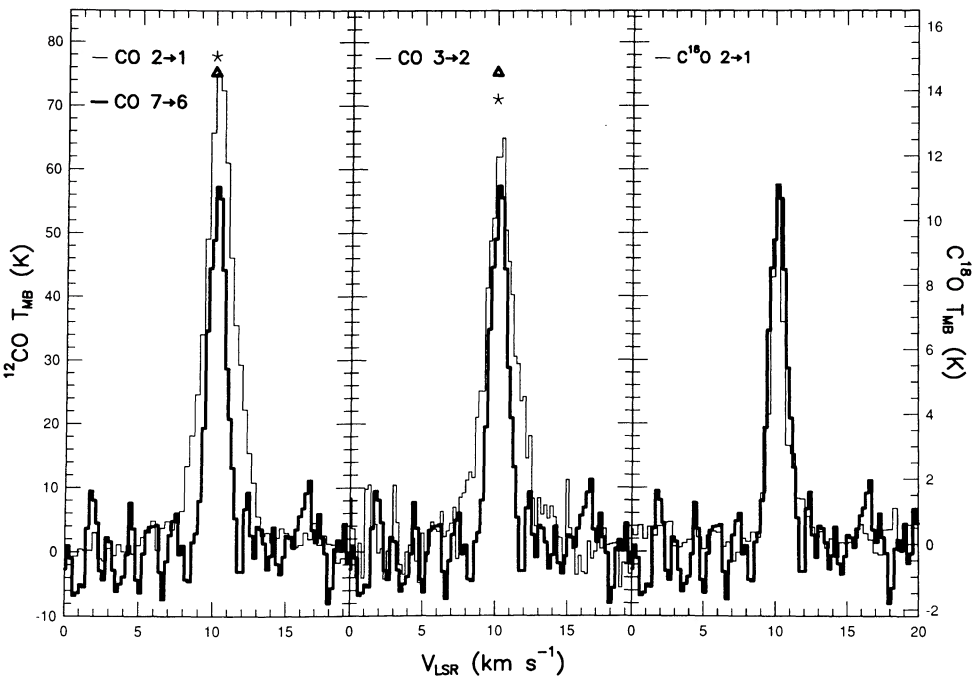

FIG. 3.—The spectrum of CO $J = 7 \rightarrow 6$ (*heavy line*) at the position 60″ east, 60″ south of HD 37903 compared with the spectra of other CO transitions (*light line*). The left vertical scale gives the Rayleigh-Jeans main beam brightness temperature. The triangle shows the Planck brightness temperature of the $7 \rightarrow 6$ line, and the star gives the Planck brightness temperature of the other transition. *Left:* CO $J = 7 \rightarrow 6$ (*heavy line*) and CO $J = 2 \rightarrow 1$. *Center:* CO $J = 7 \rightarrow 6$ (*heavy line*) and CO $J = 3 \rightarrow 2$. *Right:* CO $J = 7 \rightarrow 6$ (*heavy line*) and $C^{18}O$ $J = 2 \rightarrow 1$. The right vertical scale is for the $C^{18}O$ spectrum.

IV. DISCUSSION

a) Warm CO Gas at Inner Edge of the PDR

The detection of bright narrow line CO $7 \rightarrow 6$ emission from the ridge in NGC 2023 shows that there is warm CO in PDRs when the UV field is as low as 10^3 G_0. Since NGC 2023 is closer than most of the regions studied previously, the very good agreement between the CO $7 \rightarrow 6$, H_2, and C^+ distributions argues strongly for a common heating mechanism for the atomic and molecular PDR gas. The narrow CO $7 \rightarrow 6$ lines make shock excitation of the CO very unlikely.

The CO $7 \rightarrow 6$ emission in NGC 2023 indicates that the heating of a large column density ($\geq 10^{17}$ cm^{-2}) of CO (to $T_{gas} \geq 85$ K) in PDRs is effective even when the UV field is one or two orders of magnitude lower than in other high-J CO sources. The atomic and molecular gas distributions in the PDR are essentially identical. Allowing for beam smearing, the CO $7 \rightarrow 6$, $v = 1 \rightarrow 0$ H_2, and [C II] source sizes agree and the peak positions of the different scans agree to $\leq 20''$ ($\sim 1.5 \times 10^{17}$ cm). The temperature in the CO emission region is at least as high as the Planck brightness temperature of the $7 \rightarrow 6$ line at the peak (85 K). The kinetic temperature could be higher if the source filling factor is less than unity or if the CO $7 \rightarrow 6$ line is not optically thick, or the $J = 7$ level is not fully thermalized. The CO $7 \rightarrow 6$ measurements show that the gas temperature at the inner boundary of the emission region is substantially higher than the temperature of the far-IR emitting dust ($T_{dust} \leq 53$ K; Harvey, Thronson, and Gatley 1980). Comparison of the CO $7 \rightarrow 6$ intensity with the observed strength of the lower J CO lines does not improve the tem-

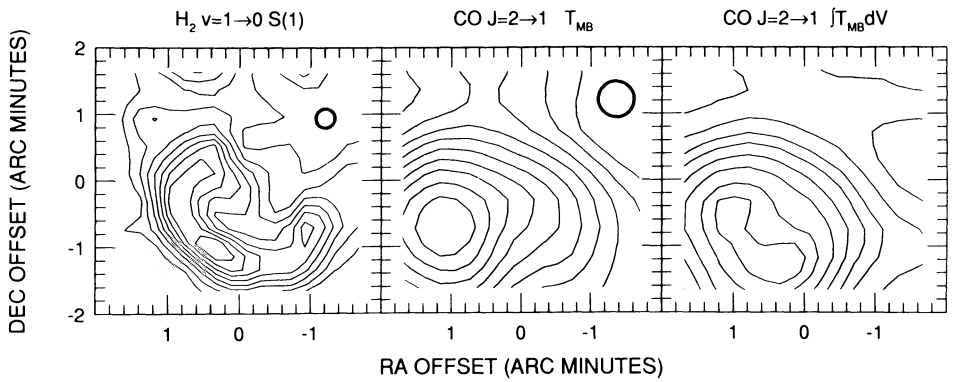

FIG. 4.—Contour maps of CO emission in NGC 2023 compared to the fluorescent H_2 emission observed by Gatley *et al.* (1987). The central position for each map is the position of HD 37903. The dark circles indicate the full width to half-maximum of the beam. *Left:* The surface brightness of the $v = 1 \rightarrow 0$ S(1) transition of H_2. Contours are 20%–90% of the peak flux of 5.4×10^{-20} W cm^{-2} in a 19″.6 beam, in 10% intervals. *Center:* Map of the peak Rayleigh-Jeans main beam brightness temperature of CO $J = 2 \rightarrow 1$. Contours are from 50%–95% of the peak $T_{MB} = 75$ K, in 5% intervals. *Right:* Map of the integrated intensity of the CO $J = 2 \rightarrow 1$ line. The peak integrated line strength is 212 K km s^{-1}. The highest contour level is 98% of the peak, the other contours are from 65% to 95% of the peak, in 5% intervals.

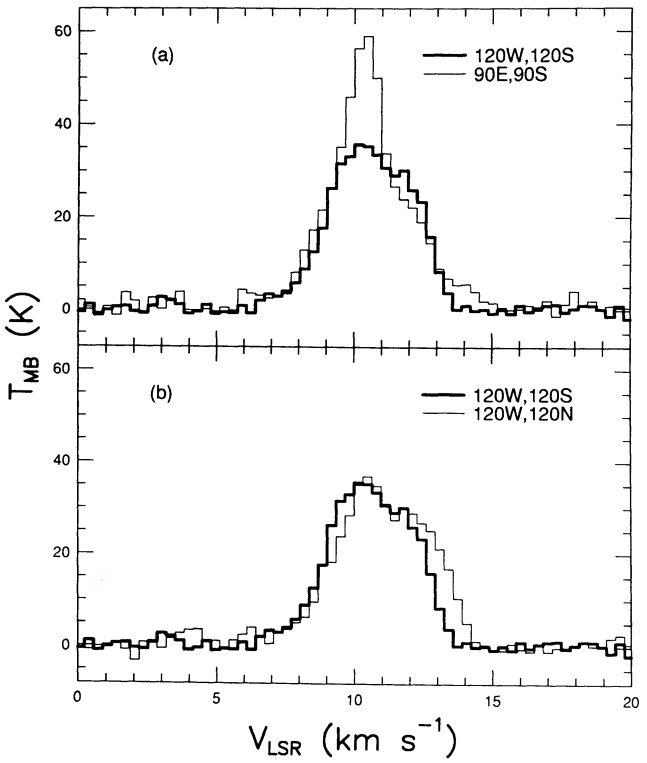

FIG. 5.—A comparison of the spectrum of ^{12}CO $J = 2 \rightarrow 1$ at several positions in NGC 2023. The position offsets are in arcseconds relative to HD 37903. The vertical scale is the Rayleigh-Jeans main beam brightness temperature of the line.

perature determination because of the large but uncertain contribution of other cloud components to the flux in the low-J lines. Based on the peak CO $7 \rightarrow 6$ brightness, the column density of CO just past the H II/neutral interface must be 1.0×10^{17} cm^{-2} or greater (this is the minimum total CO column density capable of producing the observed flux in a 1 km s^{-1} line in the $J = 7 \rightarrow 6$ transition at any combination of temperature and density [Jaffe *et al.* 1989]). If the CO emission region is as long perpendicular to the direction of our scan as it is along it, the total mass of the warm CO region is 1 $M_\odot$ or greater.

UV-photoelectric heating is sufficient to explain the observed CO-line cooling on purely energetic grounds. The luminosity of the CO $7 \rightarrow 6$ line toward the position 2.1 southeast of HD 37903 is 0.03% of the incident far-UV flux (for $G = 10^3\ G_0$). If the CO cooling in all lines is an order of magnitude larger, as estimated from radiative transfer models for a broad range of physical conditions (Harris *et al.* 1987*b*; Jaffe *et al.* 1989), a photoelectric heating efficiency of 0.3% is required to explain the CO emission. The corresponding efficiency required to account for the C^+ emission is $\sim$0.8%.

While in the more luminous sources standard photodissociation region models fail by more than an order of magnitude to produce the observed CO $7 \rightarrow 6$ line intensity at densities less than 10^6 cm^{-3} (Tielens and Hollenbach 1985*b*; Sternberg personal communication; Burton *et al.* 1989), it is possible to obtain a good match to the CO $7 \rightarrow 6$ intensity in NGC 2023 at a density in the neighborhood of $\sim 10^5$ cm^{-3} (Burton *et al.* 1989; A. G. G. M. Tielens, personal communication). Note, however, that the density in the NGC 2023 PDR must be less than a few 10^4 cm^{-3} to be consistent with the observed H_2 [$v = 1 \rightarrow 0$ $S(1)/v = 2 \rightarrow 1$ $S(1)$] intensity ratio if the currently used (and somewhat uncertain) H_2 collisional de-excitation rates are correct (Gatley *et al.* 1987; Sternberg and Dalgarno 1989). If the CO $7 \rightarrow 6$ emission region is clumpy with an area filling factor significantly smaller than unity, the PDR models could not explain the brightness temperature of the line since not enough CO would be present in the regions with sufficiently high kinetic temperatures (Burton *et al.* 1989). Differences between the hardness of the UV spectrum used in the PDR models and the hardness of actual early B star spectra may help explain for the large observed warm CO abundance. Early B stars have significantly less CO-dissociating 91.2–110 nm radiation (a factor of 2) relative to their 110–200 nm radiation, when compared with middle-late O stars (Longo *et al.* 1989) and may therefore heat the gas effectively without dissociating as much CO.

Shock excitation of the warm CO in NGC 2023 is very unlikely. While some uncertainty as to the possibility of shock excitation existed in the case of the warm CO emission from M17 SW and S106 (Harris *et al.* 1987*b*), the CO line widths seen in the warm gas in NGC 2023, 0.8 to 1.5 km s^{-1}, reflect gas motions at or below the thermal sound speed in the predominantly H_2 gas. The warm CO cannot be material behind a single shock unless the shock velocity is directly across the line of sight, since the velocities of the warm CO and the ambient cloud differ by less than 1 km s^{-1}.

b) Gas in Narrow-Line Ridge is Dense

In general, the portion of the narrow-line ridge closest to HD 37903, where the CO $7 \rightarrow 6$ emission arises, must have a density $\sim 10^5$ cm^{-3} or greater to explain the observed $7 \rightarrow 6$ line brightness (the CO $J = 7 \rightarrow 6$ transition has a critical density $\sim 6 \times 10^5$ cm^{-3}). The one possible exception would come if the kinetic temperature in the line-forming region were high ($\geq$150 K) and the column density of warm CO were very much greater than 10^{17} cm^{-2} so that radiative trapping is effective at maintaining the $J = 7$ level population at somewhat lower densities. Farther from the star, the column density derived from $C^{18}O$ $2 \rightarrow 1$ measurements implies densities greater than 5×10^4 cm^{-3} in the ridge. If the gas is clumped, the density could be larger.

c) PDR Influences Bulk of Gas in Narrow-Line Ridge

The CO $2 \rightarrow 1$, $C^{18}O$ $2 \rightarrow 1$ and CO $3 \rightarrow 2$ observations show that there is significantly more excited molecular gas immediately outside of the CO $7 \rightarrow 6/H_2/C^+$ region. The CO $2 \rightarrow 1$ Planck brightness temperature 2.1 from HD 37903 (near the $C^{18}O$ column density maximum) implies a gas temperature 80 K or greater. Like the gas close to the CO $7 \rightarrow 6$ maximum, this more distant gas is also significantly hotter than the dust. The $C^{18}O$ column density in the 1 km s^{-1} interval around 10 km s^{-1} is 9×10^{15} cm^{-2} toward the peak of the ridge. This value implies a total mass in the warm ridge material of 50–100 $M_\odot$, depending on the geometry.

d) Warm Atomic Gas is More Widespread than Warm Molecular Gas

The [C II] emission peaks on the warm narrow-line ridge, but has an overall extent similar to the broad-line plateau seen in the CO $2 \rightarrow 1$ data. The implication is that there is C^+ on the surface of the more extended broad-line cloud. This cloud may fail to produce significant CO $7 \rightarrow 6$ emission if the extended

gas is less dense and/or cooler than the ridge gas, because the critical density of the CO $J = 7 \rightarrow 6$ transition ($n_{crit} \simeq 6 \times 10^5$ cm^{-3}) is much higher than that of the [C II] $^2P_{3/2} \rightarrow {}^2P_{1/2}$ line ($n_{crit} \sim$ a few 10^3) and the energy above ground of the CO $J = 7$ level is higher than that of the C^+ $^2P_{3/2}$ level (155 K vs. 91 K). The atomic gas in the ridge itself is clearly warm and luminous. The gas temperature will be higher than the Planck brightness temperature derived in § III ($\sim$120 K), if the area filling factor of the region is less than 1 and the line opacity is also less than 1. The total cooling in the [C II] line toward NGC 2023 is 6 $L_\odot$, or $\sim$0.3% of the total luminosity reradiated by dust in this region (Emerson, Furniss, and Jennings 1975). The total mass in the C^+ region is $> 5\ M_\odot$.

e) Summary

We have explored a PDR with a known ultraviolet excitation source by examining emission from atomic and molecular material. The results have several important consequences for our understanding of these regions:

1. In agreement with models of externally excited PDRs, the photodissociation region southwest of HD 37903 contains both atomic and excited molecular material and lies closer to the exciting star than does the bulk of the molecular cloud. The C^+ emission arises closest to the star but is 1.5×10^{17} cm or less from the peaks in the excited CO and fluorescent H_2 emission regions. The $C^{18}O$ $J = 2 \rightarrow 1$ line, which traces molecular column density, has its emission peak $\sim 4 \times 10^{17}$ cm beyond the C^+ peak.

2. Even in a source with an incident UV flux as low as $\sim 10^3$ times the mean interstellar radiation field, there is a significant amount of CO $7 \rightarrow 6$ emission arising from regions with $T_{gas} >$ 85 K which is substantially greater than T_{dust}. The density of the emission region is $\sim 10^5$ cm^{-3} or more. Shock excitation of the CO responsible for this emission is very unlikely.

3. The observed bright CO $7 \rightarrow 6$ emission and the fluorescent H_2 line ratios can be explained by current PDR models with densities of $\sim 10^5$ cm^{-3} if the H_2 de-excitation rates adopted by Sternberg and Dalgarno (1989) are a factor of 2 or more too large.

4. In NGC 2023, the gas heating is also a problem in the molecular material on the outer side of the southwest ridge. At least some of this material has $T_{gas} \geq 60$ K where T_{dust} is ≤ 40 K.

We thank J. H. Black, A. G. G. M. Tielens, and A. Sternberg for helpful discussions, U. Graf, and H. Rothermel for help with the CO $7 \rightarrow 6$ observations, and the UTexas submillimeter group for help with the CO $3 \rightarrow 2$ observations. This work was supported in part by NASA grant NAG2-419 and NSF grant AST 88-15801 to the University of Texas at Austin.

REFERENCES

Black, J. H., and van Dishoeck, E. F. 1987, *Ap. J.* **322**, 412.
Burton, M., Hollenbach, D. J., and Tielens, A. G. G. M. 1989, in *Proc. 22d ESLAB Symposium, Infrared Spectroscopy in Astronomy*, ed. B. H. Kaldeich (Noordwijk: ESA), p. 141.
Chokshi, A., Tielens, A. G. G. M., Werner, M. W., and Castelaz, M. W. 1988, *Ap. J.*, **334**, 803.
Crawford, M. K., Genzel, R., Townes, C. H., and Watson, D. M. 1985, *Ap. J.*, **291**, 755.
de Boer, K. S. 1983, *Astr. Ap.*, **125**, 258.
Emerson, J. P., Furniss, I., and Jennings, R. E. 1975, *M.N.R.A.S.*, **172**, 411.
Gatley, I., *et al.* 1987, *Ap. J. (Letters)*, **318**, L73.
Genzel, R., Harris, A. I., and Stutzki, J. 1989, *Proc. 22d ESLAB Symposium, Infrared Spectroscopy in Astronomy*, ed. B. N. Kaldeich (Noordwijk: ESA), p. 115.
Habing, H. 1968, *Bull. Astr. Inst. Netherlands*, **19**, 421.
Harris, A. I. 1986, Ph.D. thesis, U. C. Berkeley.
Harris, A. I., Jaffe, D. T., Stutzki, J., and Genzel, R. 1987*a*, *Internat. J. Infrared Millimeter Waves*, **8**, 857.
Harris, A. I., Stutzki, J., Genzel, R., Lugten, J., Stacey, G. J., and Jaffe, D. T. 1987*b*, *Ap. J. (Letters)*, **322**, L49.
Harvey, P. M., Thronson, H. A., and Gatley, I. 1980, *Ap. J.*, **235**, 894.
Hildebrand, R. H., Loewenstein, R. F., Harper, D. A., Orton, G. S., Keene, J., and Whitcomb, S. E. 1985, *Icarus*, **64**, 64.
Howe, J. E., Jaffe, D. T., Stacey, G. J., and Genzel, R. 1990, in preparation.
Jaffe, D. T., Genzel, R., Harris, A. I., Lugten, J., Stacey, G. J., and Stutzki, J. 1989, *Ap. J.*, **344**, 265.
Knapp, G. R., Brown, R. L., and Kuiper, T. B. H. 1975, *Ap. J.*, **196**, 167.
Koepf, G. A., Buhl, D., Chin, D., Peck, D. D., Fetterman, H. R., Clifton, B. J., and Tannenwald, P. E. 1982, *Ap. J.*, **260**, 584.
Kutner, M., and Ulich, B. 1981, *Ap. J.*, **250**, 341.
Lee, T. A. 1968, *Ap. J.*, **152**, 913.
Lellouch, E., Encrenaz, T., and Combes, M. 1984, *Astr. Ap.*, **140**, 405.
Longo, R., Stalio, R., Polidan, R., and Rossi, L. 1989, *Ap. J.*, **339**, 474.
Maddalena, R. J., Morris, M., Moscowitz, J., and Thaddeus, P. 1986, *Ap. J.*, **303**, 375.
Pankonin, V. L., and Walmsley, C. M. 1976, *Astr. Ap.*, **48**, 341.
Racine, R. 1968, *A.J.*, **73**, 233.
Schmid-Burgk, J., *et al.* 1989, *Astr. Ap.*, **215**, 150.
Sellgren, K., Werner, M. W., and Dinerstein, H. 1983, *Ap. J. (Letters)*, **271**, L13.
Stacey, G. J., Viscuso, P., Fuller, C., and Kurtz, N. 1985, *Ap. J.*, **289**, 803.
Sternberg, A. 1988, *Ap. J.*, **332**, 400.
Sternberg, A., and Dalgarno, A. 1989, *Ap. J.*, **338**, 197.
Stutzki, J., Stacey, G. J., Genzel, R., Graf, U. U., Harris, A. I., Jaffe, D. T., Lugten, J. B., and Poglitsch, A. 1989, in *Proc. International Symposium on Submillimetre and Millimetre Astronomy*, ed. A. S. Webster (Dordrecht: Kluwer), in press.
Stutzki, J., Stacey, G. J., Genzel, R., Harris, A. I., Jaffe, D. T., and Lugten, J. B. 1988, *Ap. J.*, **332**, 379.
Tielens, A. G. G. M., and Hollenbach, D. J. 1985*a*, *Ap. J.*, **291**, 747.
———. 1985*b*, *Ap. J.*, **291**, 722.
van Dishoek, E. F., and Black, J. H. 1988, *Ap. J.*, **334**, 771.
White, G. J., Sanderson, C., Monteiro, T. S., Richardson, K. J., and Hayashi, S. S. 1989, *Astr. Ap.*, submitted.
Witt, A. N., and Schild, R. E. 1988, *Ap. J.*, **325**, 837.
Witt, A. N., Schild, R. E., and Kraiman, J. B. 1984, *Ap. J.*, **281**, 708.
Wolfire, M. G., Hollenbach, D. J., and Tielens, A. G. G. M. 1989, *Ap. J.*, **344**, 770.

R. GENZEL, A. I. HARRIS, and J. STUTZKI: Max Planck Institut für Extraterrestrische Physik, D-8046 Garching bei München, Federal Republic of Germany

J. E. HOWE and D. T. JAFFE: Department of Astronomy, R. L. Moore Hall, University of Texas at Austin, Austin, TX 78712

G. J. STACEY: Department of Physics, University of California, Berkeley, CA 94720